Evaluation of Reliability in Risk-Constrained Scheduling of Autonomous Microgrids with Demand Response and Renewable Resources

Vahedipour-Dahraie, Mostafa; Anvari-Moghaddam, Amjad; Guerrero, Josep M.

Published in:
IET Renewable Power Generation

DOI (link to publication from Publisher):
10.1049/iet-rpg.2017.0720

Publication date:
2018

Document Version
Accepted author manuscript, peer reviewed version

Evaluation of Reliability in Risk-Constrained Scheduling of Autonomous Microgrids with Demand Response and Renewable Resources

Mostafa Vahedipour-Dahraie [1*], Amjad Anvari-Moghaddam[2], Josep M. Guerrero [2]
[1] Department of Electrical and Computer Engineering, University of Birjand, Birjand, Iran.
[2] Department of Energy and Technology, Aalborg University, Aalborg, Denmark.
[*] vahedipour_m@birjand.ac.ir

Abstract: Uncertain natures of the renewable energy resources and consumers' participation in demand response (DR) programs have introduced new challenges to the energy and reserve scheduling of microgrids, particularly in the autonomous mode. In this paper, a risk-constrained stochastic framework is presented to maximize the expected profit of a microgrid operator under uncertainties of renewable resources, demand load and electricity price. In the proposed model, the trade-off between maximizing the operator's expected profit and the risk of getting low profits in undesired scenarios is modeled by using conditional value at risk (CVaR) method. The influence of consumers' participation in DR programs and their emergency load shedding for different values of lost load (VOLL) are then investigated on the expected profit of operator, CVaR, expected energy not served (EENS) and scheduled reserves of microgrid. Moreover, the impacts of different VOLL and risk aversion parameter are illustrated on the system reliability. Extensive simulation results are also presented to illustrate the impact of risk aversion on system security issues with and without DR. Numerical results demonstrate the advantages of customers' participation in DR program on the expected profit of the microgrid operator and the reliability indices.

Nomenclature

Indices

$(.)_{.,t,s}$	At time *t* in scenario *s*.
i,w,v,j	Indices of DGs, wind turbines, PV units and group of customers.
t, s	Indices of time slots and scenarios.
b, n, r	Indices of system buses.

Parameters and constants

D_j	Base load of customer *j* (kW).
β	Risk-aversion parameter.
α	Per unit confidence level.
ΔT	Time interval (hour).
$c_{w,t}$, $c_{v,t}$	Cost of wind and PV energy ($).
$c_{j,t}$	Electricity price offered to customers ($/kWh).
$c_{i,t}^{R^{up}}$ ($c_{i,t}^{R^{dn}}$)	Bid of up (down)-spinning reserve submitted by DG *i* in period *t* ($/kWh).
$c_{j,t}^{R^{up}}$ ($c_{j,t}^{R^{dn}}$)	Bid of up (down)-spinning reserve submitted by load *j* in period *t* ($/kWh).
$c_{i,t}^{R^{non}}$	Bid of non-spinning reserve submitted by unit *i* in period *t* ($/kWh).
$E_{j,t,t}$ ($E_{j,t,h}$)	Self-elasticity (cross-elasticity) of load *j*.
N_G , N_W , N_V	Number of DG, wind and PV units.
N_S , N_T , N_J	Number of scenarios, time slots and group of customers.
P_i^{max} (P_i^{min})	Maximum (minimum) generating capacity of DG *i* (kW).
D_j^{max} (D_j^{min})	Max/min load of customers' j (kW).
π_s	Probability of scenario *s*.
$G_{n,r}$ ($B_{n,r}$)	Conductance (susceptance) of line that connected node *n* to node *r*.
M_x	Set of generating units *x* (load *x*) into the set of nodes.
Λ	Set of lines.

Variables

$D_{j,t,s}^{LC}$	Involuntary load curtailment (kW).
$D_{j,t,s}^{LS}$	Involuntary load shifting (kW).
$LF_{n,r,t,s}^{P}$, ($LF_{n,r,t,s}^{Q}$)	Active (reactive) power flow from node *n* to *r* (kW).
$P_{i,t,s}$	Scheduled power for DG *i* (kW).
$P_{w,t,s}$ ($P_{v,t,s}$)	Output power of WT *w* (PV *v*) (kW).
$R_{i,t,s}^{dn}$ ($R_{j,t,s}^{dn}$)	Down-spinning reserve deployed by unit *i* (load *j*).
$R_{i,t,s}^{non}$	Non-spinning reserve deployed by DG *i*.
$L_{j,t,s}^{shed}$	Inelastic load shedding level of *j-th* load (kW).
$\delta_{n,t,s}$	Voltage angle at node *n* (rad).
$V_{n,t,s}$	Voltage magnitude (RMS value) at node *n* (pu.).
$SU_{i,t,s}$	Startup cost of DG *i* ($).
$SD_{i,t,s}$	Shute down cost of DG *i*.
$u_{i,t,s}$	Commitment status of DG *i* {0, 1}.
$y_{i,t,s}$, $z_{i,t,s}$	Startup and shutdown indicators of DG *i*.

1. Introduction

In recent years, demand-side management (DSM) has been contemplated as a crucial option in most energy policy decision-making. In restructured power systems, the scope of DSM has also been considerably expanded to include demand response (DR) programs [1]. DR programs provide many potential benefits such as reduction of operating cost

and emission [2], improvement of system reliability [3], shaping of daily load profile [4]-[5] as well as providing financial incentives to customers to benefit from lower hourly demands [6]. In addition, advent of microgrids in modern power systems has provided a high potential to facilitate the active participation of end-use consumers in DR programs [7]. However, increasing penetration level of renewable energy sources (RESs) and also, active participation of customers in DR programs increase uncertainties in the network which in turn cause imbalances between the production and consumption and deterioration of the system reliability [8]-[9]. Hence, it is necessary to efficiently manage operation of such systems in presence of uncertainties.

Value of lost load (VOLL) as an important measure in electricity market can be utilized to control the imbalances between generation and consumption [10]. VOLL can profoundly affect the voltage and frequency, spinning and non-spinning reserve (non-SR) allocation, operating costs as well as active and reactive losses of the system [11]. The level of operation security under different uncertainties can also be distinguished by the VOLL [11]. In other word, optimal selection of VOLL can result in a low-cost operation with a high level of security under the existing uncertainties in the network [12].

The uncertainties associated with RESs, electricity demand and electricity price in the day-ahead market can introduce risk into energy and reserve scheduling problem. In such condition, risk measuring plays a fundamental role in optimization under uncertainty, providing valuable information to decision makers. In some literature, risk aversion on expected cost variability is considered using conditional value-at-risk (CVaR) approach, avoiding over-conservative solutions [12-19]. For example, in [13] a risk averse profit-based optimal operation framework of a combined wind farm-cascade hydro system has been proposed in an electricity market, using hydro plants to compensate wind power forecast errors. An optimal integrated participation model has been proposed in [14], for profit enhancement of distributed resources and DR in microgrids considering system uncertainty. Moreover, a decision-making strategy for optimal pairing of wind and DR resources has proposed in [15]. The proposed strategy applied a paired resource, such as DR or storage to mitigate the generation scheduling errors inherited in stochastic technologies. In [16], a decision making model has been proposed for coordinated operation of wind power producers and DR aggregators participating in the day-ahead market. A minimum CVaR term has been also included in the model formulation to account for the uncertainty around the true outcomes of day-ahead prices and wind energy. Moreover, in [17], a risk-constrained stochastic programming framework has been proposed, to maximize the profit of microgrid aggregators with considering responsive loads. Authors of [18] has proposed a scenario-based two-stage stochastic programming model to jointly optimize the scheduling of several options in a microgrid, including DR, RESs and energy storage devices. In [19], authors have proposed a bi-level framework for the problem of decision-making by an EV aggregator in a competitive environment. In the same work, CVaR is applied in the decision-making process to confront the uncertainties in day-ahead and balancing markets. Moreover, in [20], authors have presented a risk-constrained two-stage stochastic programming model from an islanded microgrid operator's perspective for energy and reserve scheduling considering risk management strategy. However, in none of the reviewed literature, the effects of VOLL indices on reliability issues of an autonomous microgrid have been reported.

In this study, a risk-constrained stochastic programming framework is presented for optimal scheduling of an autonomous microgrid under uncertainties. Based on this program, microgrid operator procures energy from local distributed generation (DG) units and RESs to supply microgrid customers. The objective is to maximize the expected profit of the system operator through optimal scheduling of resources considering risk aversion and system reliability issues. To deal with various uncertainties, a risk-constrained two-stage stochastic programming formulation is proposed. An efficient solution strategy based on Benders' decomposition is also developed to solve the proposed reliability based optimization problem under uncertainty. As a whole the main contributions of this paper are as follows:

1) A risk-constrained two-stage stochastic programming formulation is proposed to represent the underlying optimization problem where the risk aversion of the microgrid operator is captured by using the CVaR approach,
2) A model for joint energy and reserve scheduling is presented by considering reliability issues as well as RESs and DR uncertainties that can be easily adopted by other entities such as a load serving entity (LSE), a retailer, or a distribution company (DISCO),
3) An efficient framework is proposed to illustrate the impacts of different VOLL and risk aversion parameter on system reliability.

The rest of paper is arranged as follows: In section 2, system model is explained. In section 3, the proposed risk-neutral stochastic optimization formulation is described. The proposed method for solving the scheduling problem is presented in section 4. Case studies together with simulation results are presented in section 5. Finally, section 6 draws the conclusions.

2. System Model Description

In this study, a medium-scale residential autonomous microgrid is considered with an average hourly load in the range of hundred kilowatts. It has several DGs such as micro-turbines, fuel cells and RESs such as wind and PV units. A simplified graphical description of the proposed model is shown in Fig. 1. In this model, the microgrid operator has a take-or-pay contract [21] to buy energy from various energy sources while it sells electricity to customers under real-time pricing scheme, which is based on a service agreement. Customers are also able to respond to electricity prices by adjusting their loads to reduce consumption costs. To do so, it is assumed that the customers are equipped with house energy management controllers (Hex MCs) and several smart household appliances. Due to geographically diverse consumers, N_J groups of loads are also considered for evaluating the influence of users' participation in DR

programs. Moreover, the system operator has access to the required information such as wind speed, solar irradiation, electricity price, generation unit and network information for the scheduling horizon. The energy and reserve scheduling is done in a way to maximize the operator's expected profit and to minimize the users' energy consumption costs while fulfilling the microgrid security and technical constraints. Also, reliability of the microgrid in a risk-constrained scheduling is evaluated with and without DR participation.

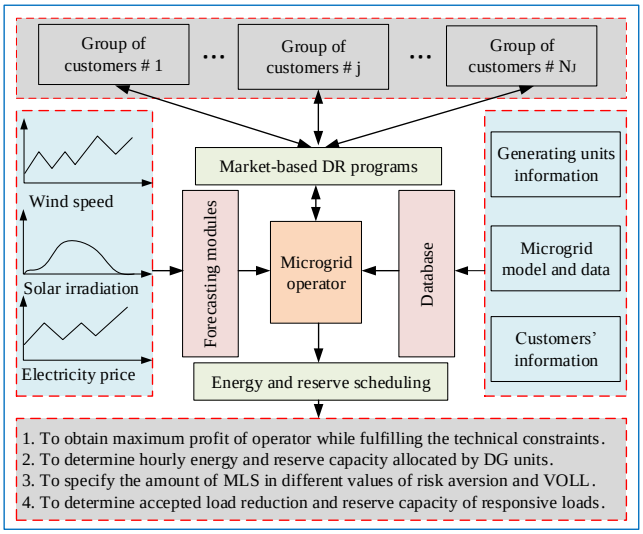

Fig. 1. *Schematic representation of the proposed model.*

3. Risk-Neutral Stochastic Optimization Formulation

3.1. Incorporating Risk Management

In financial risk management, Value-at-Risk (VaR) is a widely-used risk measure focusing on the down-side (i.e., tail) risk [22]. However, VaR is not a coherent risk measure. VaR is only coherent when the underlying loss distribution is normal, otherwise it lacks sub-additively. Also, VaR measure does not give any information about potential losses in the $(1-\alpha)$ worst cases, thus calculating VaR optimal portfolios can be difficult or even impossible [23]. The Conditional Value-at-Risk (CVaR) is closely linked to VaR, but provides several distinct advantages especially when the loss distribution is not normal or when the optimization problem is high-dimensional (as the case we experienced in this work). Furthermore, in settings where an investor/system operator wants to form a portfolio of different assets, the portfolio CVaR can be optimized by a computationally efficient, linear minimization problem, which simultaneously gives the VaR at the same confidence level as a by-product. Bearing all this in mind, the CVaR measure for a discrete distribution and at a given confidence level α is defined mathematically as [22, 23]:

$$CVaR = \max_{\xi,\eta_s}\left(\xi - \frac{1}{1-\alpha}\sum_{s=1}^{N_S}\pi_s.\eta_s\right) \tag{1}$$

Subject to:

$$\eta_s + profit_s - \xi \geq 0; \qquad \eta_s \geq 0 \tag{2}$$

where, α is the confidence level, $profit_s$ is the profit in scenario s, π_s is probability of scenario s and η_s is an auxiliary nonnegative variable equals to the difference between auxiliary variable ξ and the $profit_s$ when the $profit_s$ is smaller than ξ.

Based on (1), if all profit scenarios are equiprobable, CVaR is computed as the expected profit in the $(1-\alpha)\times 100\%$ worst scenarios. Therefore, CVaR at a given confidence level α is defined as the expected value of the profit smaller than (1-α)-quantile of the profit distribution. In fact, in the proposed scenario-based stochastic optimization method, α-CVaR represents approximately the expected profit of the (1-α)×100% scenarios yielding the lowest profits.

3.2. Objective Function

The objective of microgrid operator is to maximize its expected profit in an uncertain environment. Therefore, a risk-constrained two-stage stochastic programming framework using α-CVaR method is proposed to formulate the objective function. In this regard, the weighted α-CVaR value of the profit is added to a risk-neutral optimization problem through a weighting parameter called risk aversion factor β. Therefore, the objective is to maximize the expected profit of the microgrid operator as follows:

$$Max \quad \sum_{s=1}^{N_s}\pi_s.profit_s + \beta.CVaR \tag{3}$$

where the $profit_s$ in scenario s is defined as:

$$\begin{aligned} profit_s = \sum_{t=1}^{N_T}\Delta T.\Bigg\{\sum_{s=1}^{N_S}\pi_s.\Bigg[&\sum_{j=1}^{N_J}c_{j,t}.(D_{j,t,s} - D_{j,t,s}^{LC} - D_{j,t,s}^{LS} - L_{j,t,s}^{Shed}) \\ &- \sum_{i=1}^{N_G}[C(P_{i,t,s}) + SU_{i,t,s}. + SD_{i,t,s}] - \sum_{w=1}^{N_W}c_{w,t}.P_{w,t,s} - \sum_{v=1}^{N_V}c_{v,t}.P_{v,t,s} \\ &- \sum_{i=1}^{N_G}(c_{i,t}^{R^{up}}.R_{i,t,s}^{up} + c_{i,t}^{R^{non}}.R_{i,t,s}^{non} - c_{i,t}^{R^{dn}}.R_{i,t,s}^{dn}) - \sum_{j=1}^{N_J}(c_{j,t}^{R^{up}}.R_{j,t,s}^{up} - c_{j,t}^{R^{dn}}.R_{j,t,s}^{dn}) \\ &- \sum_{j=1}^{N_J}(C_{j,t,s}^{LS} + C_{j,t,s}^{LS} + VOLL\times L_{j,t,s}^{shed})\Bigg]\Bigg\} \end{aligned} \tag{4}$$

The objective function is the sum of the revenues obtained from selling electricity to the microgrid customers, minus the operating cost of DG units (including the cost of purchasing energy from DGs and their start-up/down cost), the cost of purchasing energy from wind and PV units, the cost of reserves allocated to DGs and responsive loads as well as the payments for the LC and LS and also mandatory load shedding (MLS). Note that the first line of objective function represents the base load of group j, minus the involuntary and mandatory load curtailment. Also, the last line represents the payment to customers for their participation in the involuntary load shedding or load curtailment as well as the cost of expected load not served for the inelastic loads in working scenarios. In this study, it is assumed that wind and PV units are not owned by the microgrid operator, so they are paid a cost-based price for the electricity they supply to the grid.

3.3. Constraints of the Problem

The proposed objective function is subject to the following constraints:

1) Active and reactive power balance: Power supplied from committed units and renewable resources must satisfy the load demand.

$$\sum_{i:(i,n)\in M_I(t,s)} P_{i,t,s} + \sum_{w:(w,n)\in M_W(t,s)} P_{w,t,s} + \sum_{v:(v,n)\in M_V(t,s)} P_{v,t,s} = \sum_{j:(j,n)\in M_L(t,s)} (D_{j,t,s} - D^{LC}_{j,t,s} - D^{LS}_{j,t,s} - L^{shed}_{j,t,s}) + \sum_{r:(n,r)\in\Lambda(t,s)} LF^{P}_{n,r,t,s} \quad ((5)$$

$$\sum_{i:(i,n)\in M_I(t,s)} Q_{i,t,s} + \sum_{w:(w,n)\in M_W(t,s)} Q_{w,t,s} + \sum_{v:(v,n)\in M_V(t,s)} Q_{v,t,s} = \sum_{j:(j,n)\in M_L(t,s)} (Q_{j,t,s} - Q^{LC}_{j,t,s} - Q^{LS}_{j,t,s} - Q^{shed}_{j,t,s}) + \sum_{r:(n,r)\in\Lambda(t,s)} LF^{Q}_{n,r,t,s} \quad (6)$$

Equations (5)-(6) describe the constraints of active and reactive power balance on bus n at time t and scenario s. The last terms of these equations stand for the active and reactive power flow from bus n to bus r represented by (7) and (8), respectively.

$$LF^{P}_{n,r,t,s} = G_{n,r}\left[V^2_{n,t,s} - V_{n,t,s}.V_{r,t,s}\cos(\delta_{n,t,s} - \delta_{r,t,s})\right] - B_{n,r}.V_{n,t,s}.V_{r,t,s}\sin(\delta_{n,t,s} - \delta_{r,t,s}) \quad (7)$$

$$LF^{Q}_{n,r,t,s} = -B_{n,r}\left[V^2_{n,t,s} - V_{n,t,s}.V_{r,t,s}\cos(\delta_{n,t,s} - \delta_{r,t,s})\right] - G_{n,r}.V_{n,t,s}.V_{r,t,s}\sin(\delta_{n,t,s} - \delta_{r,t,s}) \quad (8)$$

Moreover, equations (9)-(12) represent voltage magnitude limits, line power flow bounds, emergency load curtailment limits, and limits of reactive power of DGs.

$$V^{\min}_n \le V_{n,t,s} \le V^{\max}_n \quad (9)$$

$$-LF^{\max}_{n,r} \le \sqrt{\left(LF^{P}_{n,r,t,s}\right)^2 + \left(LF^{Q}_{n,r,t,s}\right)^2} \le LF^{\max}_{n,r} \quad (10)$$

$$0 \le L^{shed}_{j,t,s} \le L_{j,t} \quad (11)$$

$$Q^{\min}_i \le Q_{i,t,s} \le Q^{\max}_i \quad (12)$$

2) Operation Constraints for DG units: The following constraints should be met for DGs in each scenario [24]:

$$C(P_{i,t,s}) = A_i.u_{i,t,s} + \sum_{m=1}^{N_i} \lambda_{i,m}.P_{i,m,t,s} \quad (13)$$

$$P_{i,t,s} = P^{\min}_i.u_{i,t,s} + \sum_{m=1}^{N_i} P_{i,m,t,s}; \qquad 0 \le P_{i,m,t,s} \le P_{i,m} \quad (14)$$

Constraint (13) captures the generation cost of DG units that is approximated by piecewise linear functions [24]. Moreover, output power of DG units obtained by (14). In these equations, m denotes the indices of segments and N_i represents the number of segments in the cost function of unit i, and A_i is the cost of running unit i at its minimum power generation. Moreover, $\lambda_{i,m}$ is the marginal cost associated with segment m of cost function unit i, $P_{i,m}$ is the upper limit of power generation from the m-th segment of cost function of unit i and $P_{i,m,t,s}$ is power generation of unit i from the m-th segment at time t in scenario s.

$$SU_{i,t,s} \le CU_i.y_{i,t,s}; \qquad SD_{i,t,s} \le CD_i.z_{i,t,s} \quad (15)$$

$$P_{i,t,s} - P_{i,t-1,s} \le UR_i.(1 - y_{i,t,s}) + P^{\min}_i.y_{i,t,s} \quad (16)$$

$$P_{i,t-1,s} - P_{i,t,s} \le DR_i.(1 - z_{i,t,s}) + P^{\min}_i.z_{i,t,s} \quad (17)$$

$$\sum_{h=t}^{t+UT_i-1} u_{i,t,s} \ge UT_i.y_{i,t,s} \quad (18)$$

$$\sum_{h=t}^{t+DT_i-1} (1 - u_{i,t,s}) \ge DT_i.z_{i,t,s} \quad (19)$$

$$y_{i,t,s} - z_{i,t,s} = u_{i,t,s} - u_{i,t-1,s}; \qquad y_{i,t,s} + z_{i,t,s} \le 1 \quad (20)$$

Constraint (15) represents the limit of the start-up and shut-down costs of DGs in each scenario. Also, constraints (16)-(20) denote the limits on ramping rates, minimum ON/OFF duration, and relationship between binary variables [24]. Note that UR_i and DR_i are the ramping-down and ramping-up rates limit of unit i and UT_i and DT_i are the minimum up and down time of unit i.

In other to fully regulate the frequency, the active power generation of DGs should be adjusted with respect to the changes of customers' consumption. These adjustments should be done in accordance with active power production ramp rates, power capacity limits and reserve constraints. The limits of up, down and non-SRs of DGs are represented by (21)-(23).

$$0 \le R^{up}_{i,t,s} \le P^{\max}_i u_{i,t,s} - P_{i,t,s} \quad (21)$$

$$0 \le R^{dn}_{i,t,s} \le P_{i,t,s} - P^{\min}_i u_{i,t,s} \quad (22)$$

$$0 \le R^{non}_{i,t,s} \le P^{\max}_{i,t,s}(1 - u_{i,t,s}) \quad (23)$$

3) Demand-side constraints: These constraints determine the degree of participation of each group of customers in energy and reserve scheduling. For each group of customers the following criteria must be met:

$$D^{\min}_{j,t} \le D_{j,t,s} \le D^{\max}_{j,t} \quad (24)$$

$$0 \le R^{up}_{j,t,s} \le D_{j,t,s} - D^{\min}_{j,t} \quad (25)$$

$$0 \le R^{dn}_{j,t,s} \le D^{\max}_{j,t} - D_{j,t,s} \quad (26)$$

4) Relationship between scheduled and deployed reserves: The relationship between the DG units scheduled and deployed reserves limits are represented by (27)-(29).

$$0 \le r^{up}_{i,t,s} \le R^{up}_{i,t,s} \quad (27)$$

$$0 \le r^{dn}_{i,t,s} \le R^{dn}_{i,t,s} \quad (28)$$

$$0 \le r^{non}_{i,t,s} \le R^{non}_{i,t,s} \quad (29)$$

Similarly, the relationship between the responsive loads scheduled and deployed reserves limits are represented by (30)-(31).

$$0 \le r^{up}_{j,t,s} \le R^{up}_{j,t,s} \quad (30)$$

$$0 \le r^{dn}_{j,t,s} \le R^{dn}_{j,t,s} \quad (31)$$

5) Linking constraints: These constraints relate market decisions to the real-time operation of the microgrid through the deployment of reserves provided by DG units and

responsive loads. The constraints (32)-(33) couple the first stage decisions with possible realizations of stochastic processes.

$$P_{i,t,s} = P_{i,t} + r_{i,t,s}^{up} + r_{i,t,s}^{non} - r_{i,t,s}^{dn} \tag{32}$$

$$D_{j,t,s} = D_{j,t} - r_{j,t,s}^{up} + r_{j,t,s}^{dn} \tag{33}$$

3.4. Economic Model of DR

The consumers' loads are generally divided into three categories: shiftable, sheddable and non-sheddable loads. Sheddable loads are those that can be curtailed or turned-off by the consumer or the system operator without causing any disruption to the lives, security issues or irreparable harms. Shiftable loads are related to such consumption units that must be run in the course of a day; however, there is no specific run time for them. Therefore, customers participate in DR program using two general categories of electrical devices including sheddable and shiftable loads by using load curtailment (LC) and load shifting (LS) options, respectively [25]. An economic model for the participation of customers in DR programs can be developed based on user's load reduction in terms of LC/LS mechanisms. However, the amount of load reduction depends on the demand elasticity of customers and electricity prices. Demand elasticity is defined as demand sensitivity to the price signal. It is comprised of self-elasticity and cross-elasticity coefficients. Self-elasticity represents changes in demand due to changes in price at the same time instant t and can be written as [26]:

$$E_{j,t,t} = \frac{c_{j,t}^{\text{int}}}{D_{j,t}^{\text{int}}} \cdot \frac{\partial D_{j,t}}{\partial c_{j,t}} \tag{34}$$

where, $D_{j,t}^{\text{int}}$ is the initial value of demand associated with customers of group *j* and $c_{j,t}^{\text{int}}$ is the initial value of electricity price. In this way, LC can be represented by self-elasticity. By the same token, LS can be represented by cross-elasticity which denotes the consumer's multi-period sensitivity with respect to the price. To achieve maximum benefit, each group of customers applies both LC and LS options and changes their consumption from $D_{j,t}^{\text{int}}$ to $D_{j,t}$ in period *t* as:

$$D_{j,t} = D_{j,t}^{\text{int}} + \Delta D_{j,t} \tag{35}$$

The benefit of group *j* can be calculated as:

$$S(D_{j,t}) = B(D_{j,t}) - D_{j,t} . c_{j,t} \tag{36}$$

where, $S(D_{j,t})$ and $B(D_{j,t})$ represent benefit and income of group *j* at period t after implementing DR program. To maximize the benefit of group *j*, the following criteria must be met:

$$\frac{\partial S(D_{j,t})}{\partial D_{j,t}} = \frac{\partial B(D_{j,t})}{\partial D_{j,t}} - c_{j,t} = 0 \tag{37}$$

Among commonly-used functions, the quadratic form is the most pessimistic model and the most usual customers' utility function [26]. Based on a quadratic model of DR, the utility of group *j* of customers is obtained as [26]:

$$B(D_{j,t}) = B_{j,t}^{0} + \frac{c_{j,t} . D_{j,t}}{1 + E_{j,t,t}^{-1}} \times \left[\left(\frac{D_{j,t}}{D_{j,t}^{\text{int}}} \right)^{E_{j,t,t}^{-1}} - 1 \right] \tag{38}$$

Differentiating (38) with respect to $D_{j,t}$ and substituting into (37) gives:

$$(1 + E_{j,t,t}^{-1}) . \left(\frac{c_{j,t}^{\text{int}}}{c_{j,t}} \right) = \frac{D_{j,t}}{D_{j,t}^{\text{int}}} + E_{j,t,t}^{-1} . \left(\frac{D_{j,t}}{D_{j,t}^{\text{int}}} \right)^{E_{j,t,t}^{-1}} - 1 \tag{39}$$

Therefore, the consumption of group *j* at time *t* is obtained as follows:

$$D_{j,t} = D_{j,t}^{\text{int}} . \left[\frac{c_{j,t}}{c_{j,t}^{\text{int}}} + \frac{1}{1 + E_{j,t,t}^{-1}} \right]^{E_{j,t,t}^{-1}} - 1 \tag{40}$$

Furthermore, the amount of demand after DR using cross-elasticity [26], which modeled LS option, can be obtained as:

$$D_{j,t} = D_{j,t}^{\text{int}} . \prod_{\substack{t=1 \\ t \neq h}}^{N_T} \left[\frac{c_{j,t}}{c_{j,t}^{\text{int}}} + \frac{1}{1 + E_{j,t,t}^{-1}} \right]^{E_{j,t,t}} \tag{41}$$

When the customers of group *j* participate in DR using both LC and LS options, the total demand can be calculated as:

$$D_{j,t} = D_{j,t}^{\text{int}} . \exp \sum_{h=1}^{N_T} E_{j,t,t} . \ln \left[\frac{c_{j,t}}{c_{j,t}^{\text{int}}} + \frac{1}{1 + E_{j,t,t}^{-1}} \right] \tag{42}$$

4. Proposed Solution Methodology

Fig. 2 illustrates the flowchart of the proposed method for solving the optimal scheduling problem in a microgrid. This flowchart has three stages. In the first stage, the structure of demand that is specified by customers' electrical devices and equipment is determined. After customers' registration, their total loads are categorized as shiftable, sheddable and non-sheddable loads and are considered as input data for the next stage. In the second stage scenario generation and reduction process is done for stochastic parameters. In this regard, forecasting errors of stochastic variables are modeled as continuous probability density functions (PDF) with a zero-mean normal distribution and different standard deviations. Monte Carlo simulation (MCS) and roulette wheel mechanism (RWM) are also used to generate a large number of scenarios representing the uncertain parameters based on their corresponding PDFs over the examined period [27]. Each scenario captures the information of the hourly wind speed, the hourly irradiation and the hourly load in the operating day. It should be noted that the selection of an appropriately sized set of scenarios has been done based on a trade-off between tractability issues and problem representation issues using the sample average approach method detailed in [28]. To mitigate the computational burden of the stochastic procedure, K-means algorithm [29] is then applied to reduce the number of scenarios into a smaller set representing well enough the uncertainties. Finally, the proposed optimization model is solved by employing a risk-constraints stochastic programming approach for each scenario. In this stage, the reduced scenarios are applied to the proposed model to maximize the expected profit of islanded MG while considering system security constraints and reliability issues. As shown, the solution method includes a master problem and a sub-problem in which Benders decomposition (BD) theory [30] is applied for problem

solving. In the master problem, unit commitment (UC), economic dispatch and also the amount LC/LS in DR programs are determined in a MIP-based problem. Sub-problem solves, instead, a nonlinear programming problem representing hourly AC security-constrained optimal power flow. The solution generated by the upper layer (master problem) is then considered in the sub-problem and the feasibility and optimality of the optimal decision of base case decisions is evaluated under system contingencies to detect flow violations. If sub-problem fails to get a feasible solution, an infeasibility cut based on the BD theory is created accordingly and included to the master problem to recalculate the dispatch and hourly commitment states of the generating units and also responsive loads condition.

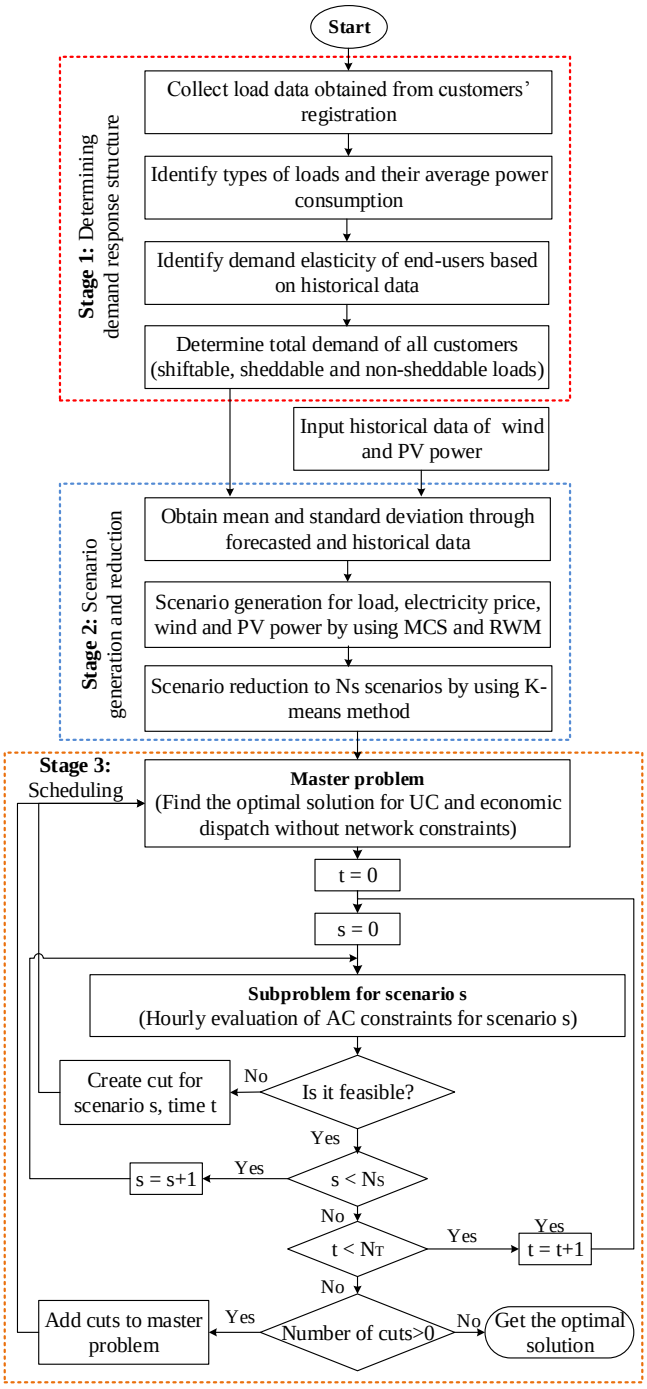

Fig. 2. Flowchart of the proposed solution methodology.

5. Simulation and Numerical Results

5.1. Case Study

The low-voltage autonomous microgrid, as shown in Fig. 3, is considered in order to demonstrate the effectiveness of the proposed approach. The mass flow of data that is exchanged between the local controllers (LCs), (Hex MCs) and the energy management controller (EMC) as well as the power flow direction are shown. Moreover, in the proposed scheme DR consists of fully automated signaling from a utility (which is the microgrid operator in our case) to provide automated connectivity to end-use customers' control systems and strategies. The microgrid has five controllable DG units including two micro-turbines (MT1 & MT2), two fuel cells (FC1 & FC2), and one gas engine (GE) with the technical information given in [20]. Additionally, three similar wind turbines, each with a capacity of 80 kW and two similar PV plants, each with a capacity of 70 kW are considered in the examined microgrid. The detailed data regarding the operating range of the units and their energy and reserve costs are given in Table 1, [20], [31]. The microgrid feeds eight groups of aggregated loads that are equipped with proper controllers to participate in DR programs. The hourly total load, output power of wind and PV units and also the hourly electricity price in different scenarios for one day are shown in Fig. 4. The dashed blue lines in this figure show the mean of each stochastic parameter that are equivalent to the forecasted values of related variable which extracted from [20], [31]. The PDF of each stochastic parameter is calculated based on previous records of that parameter for the examined environment. Here, the PDFs are divided into seven discrete intervals with different probability levels. It should be mention that real-time pricing tariff adopted in this study is obtained based on the stability margin index (SMI) concept that is proposed in [32] by the authors. Also, standard deviation of the wind power, PV power, electricity price and load demand forecast errors are ±10%, ±10%, ±15%, and ±20%, respectively [31]-[33].

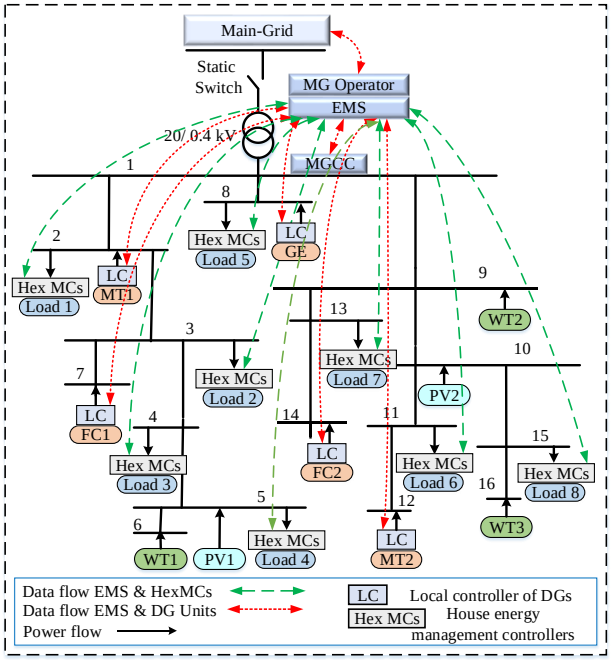

Fig. 3. Single line diagram of the studied microgrid.

Table 1 Data of range of units' production and their energy and reserve costs.

Unit	Min-Max generation capacity (kW)	Marginal cost ($/kWh)	Start-up cost ($)	Shut-down cost ($)	Cost of up-SR ($)	Cost of down-SR ($)	Cost of non-SR ($)
MT_1	25-150	0.055	0.090	0.080	0.031	0.030	0.030
MT_2	25-150	0.068	0.090	0.080	0.031	0.030	0.030
FC_1	20-100	0.120	0.160	0.090	0.038	0.035	0.035
FC_2	20-100	0.142	0.160	0.090	0.038	0.035	0.035
GE	35-150	0.084	0.120	0.080	0.039	0.037	0.035
WT	0-80	0.055	-	-	-	-	-
PV	0-70	0.065	-	-	-	-	-

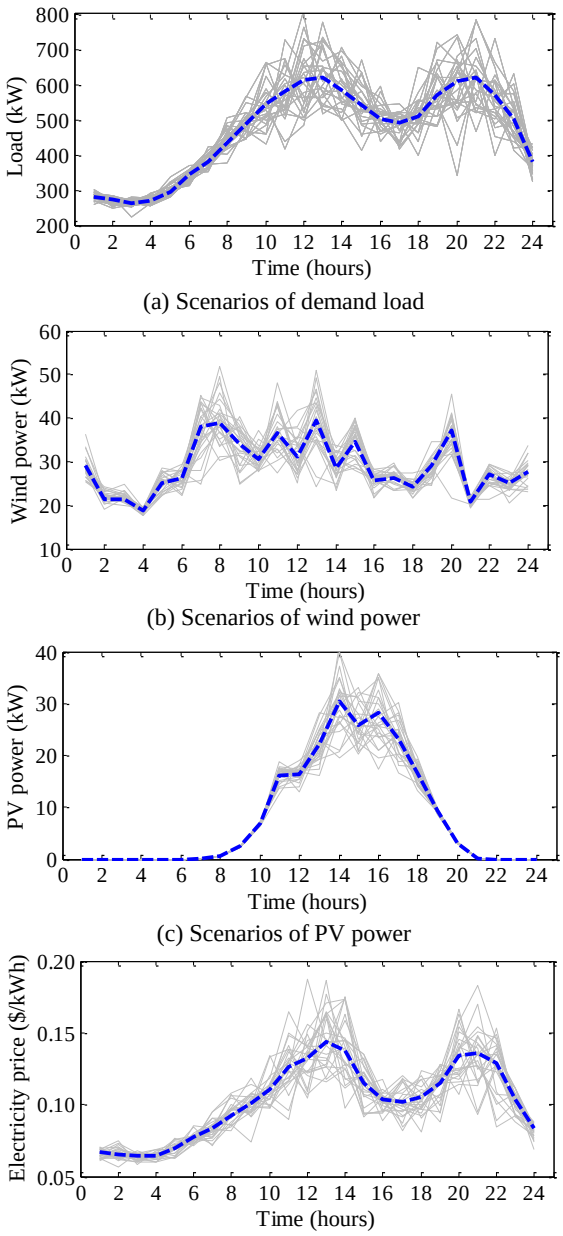

(a) Scenarios of demand load

(b) Scenarios of wind power

(c) Scenarios of PV power

(d) Scenarios of electricity price

Fig. 4. *Scenarios(grey lines) and the mean (dashed blue lines) of each stochastic parameter*

A number of 2000 initial scenarios are generated using MCS and RWM strategies to model the forecasting errors. Then, K-means algorithm is implemented to reduce the initial scenarios into a set of 25 selected scenarios that represent well enough the uncertainties. The real-time pricing tariff obtained based on the proposed method in [32], is used to encourage the customers to participate in DR programs. Also, the total load has been created by aggregating the demands of 200 residential homes. The type of sheddable and shiftable loads and their average power consumption level for one residential home are illustrated in Tables 2 and 3, respectively [25].

In this study, the scheduling horizon is considered one day which is divided into 24 equal time slots. Finally, the reduced scenarios are applied to a risk-constrained two-stage optimization model to maximize the expected profit of microgrid operator. The optimization is carried out by CPLEX solver using GAMS software [34] on a PC with 4 GB of RAM and Intel Core i7 @ 2.60 GHz processor.

Table 2 Type of sheddable loads and their average power consumption level for one residential home.

(h)	Sheddable loads	Power (W)	(h)	Sheddable loads	Power (W)
1	Group A*	200	13	Group B	1550
2	Group A	200	14	Group B	1300
3	Group A	200	15	Group B	1300
4	Group A	200	16	Group B	1300
5	Group A	200	17	Group B	1550
6	Group A	200	18	Group B	1550
7	Group B**	1300	19	Group B	1550
8	Group B	1550	20	Group B	1550
9	Group B	1550	21	Group B	1550
10	Group B	1550	22	Group B	1550
11	Group B	1550	23	Group B	1300
12	Group B	1550	24	Group B	1300

* Group A: Electrical equipment up to 200W

**Group B: Fans, air conditioners, computers, hairdryer, coolers, extractor hoods, and other electrical equipment up to 1000W

Table 3 Type of shiftable loads and their average power consumption level for one residential home.

Type of shiftable load	Average power (W)	Type of shiftable load	Average power (W)
Vacuum cleaners	1200	Dishwashers	2000
Washing machines	2500	Meat grinders	1000
Dryers	1800	Irons	1000

5.2. Numerical Results

The expected profit of the microgrid operator versus CVaR for different levels of risk aversion with and without DR is shown in Fig. 5. Here, the confidence level to compute CVaR is considered 95% in all instances. To avoid crowding data, the optimal solution of the maximization problem is obtained only for 13 values of β by modifying risk aversion parameter from 0.01 to 2 as shown in the figure. Risk aversion parameter models the trade-off between the expected profit and the profit variability (measured in terms of CVaR). The efficient frontiers are obtained for two amounts of VOLL =1 \$/kWh and 5 \$/kWh to demonstrate the effects of VOLL. As shown, by increasing β, CVaR increases and the operator's expected profit decreases in all cases. At the first point (e.g., β =0.01), which shows a solution with a near-zero risk aversion, the maximum profit at the minimum CVaR is attained. By increasing β, the total expected profit decreases, however the average expected profit of the worst-case scenarios increases, thus, the risk exposure is mitigated. Moreover, comparison of results in different cases in the same figure shows that with increasing β, when customers participate in DR program, the rate of decrement in the expected profit is lower than that of in case without DR. Also, as observed, when β increases from 0.01 to 0.1, although the profit does not change so much, CVaR rises substantially. With further increase of β, the operator's expected profit will be significantly reduced, however CVaR will not be changed so much. In case of without DR and VOLL=1 \$/kWh, the expected profit and CVaR varies from \$287.07 and \$113.41 for β = 0 to \$281.08 and \$168.13 for β = 2, respectively. It shows a reduction of 2.1% in the expected profit and a 48.2% increase in the CVaR. In case with DR and VOLL=1 \$/kWh, the expected profit and CVaR varies from \$391.97 and \$308.84 for β = 0.01 to \$374.65 and \$337.96 for β = 2, respectively, that shows a reduction of 4.4% in the expected profit and a 9.4% increase in the CVaR. When customers participate in DR, the uncertainty in system environment increases which in turn necessitate more reserve allocation in higher values of β. Hence, the operator encounters lower expected profit by increasing of β. Moreover, by increasing the reserve allocation, the MLS in undesired scenarios is reduced and consequently, the increment percentage of CVaR decreases.

Fig. 6 shows the expected profit and cost of expected energy not served (EENS) under different VOLL values in cases with and without DR actions. As shown in this figure, without DR, the cost of EENS (payment to customers for their MLS) increases by increasing VOLL values. Although, with increasing VOLL the EENS reduces severely, the product of VOLL and expected EENS increases. Moreover, for higher values of VOLL, additional SR is much more cost-effective than the MLS imposed on consumers. Also, in higher VOLL values, the expensive generating units are committed to reduce the MLS. Therefore, by increasing the VOLL, the operator's expected profit reduces in case without DR, and even it may be negative (profit losses) when considered higher values for VOLL. Moreover, in case with DR support as shown in Fig. 6 (b), demand of peak periods is decreased by LC/LS activities and as the result the MLS (as well as the cost of EENS) reduces in peak hours. Comparison of the results in Fig. 6 (a) and (b) shows that with customers' participation in DR program the operator's expected profit is increased, especially in higher values of VOLL.

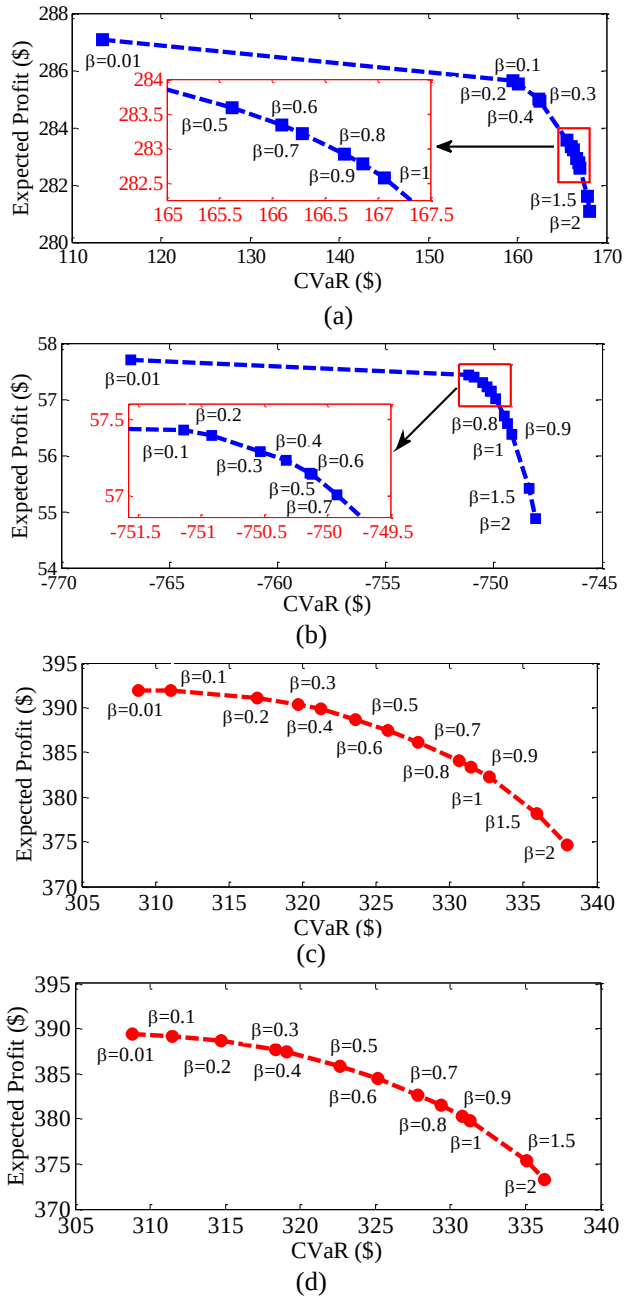

Fig. 5. *Operator's expected profit versus CVaR*
(a) without DR, VOLL=1 \$/kWh
(b) without DR, VOLL=5 \$/kWh
(c) with DR, VOLL=1 \$/kWh
(d) with DR, VOLL=5 \$/kWh

The expected profit versus CVaR for different values of VOLL at the constant β (i.e., β = 0.01) is shown in Fig. 7. It is observed that with increasing VOLL both values of expected profit and CVaR decrease in two cases. Without DR support, a reduction of 187.4% in the expected profit is observed, however, in case with DR, this value is 24.1%. Moreover, with the support of responsive loads in peak periods and their contributions in better reserve allocation, the MLS associated with undesired scenarios and consequently the cost of EENS is decreased substantially.

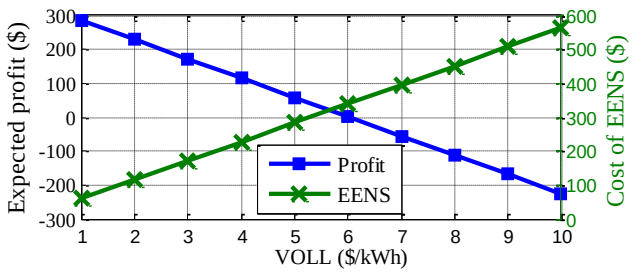

(a)

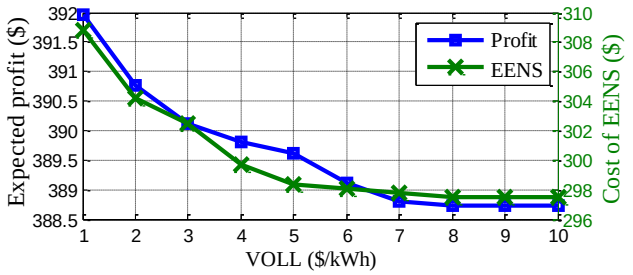

(b)

Fig. 6. *Operator's expected profit and cost of EENS under different VOLL values*
(a) without DR and **(b)** with DR.

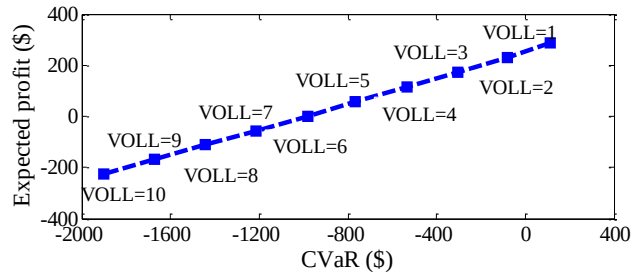

(a)

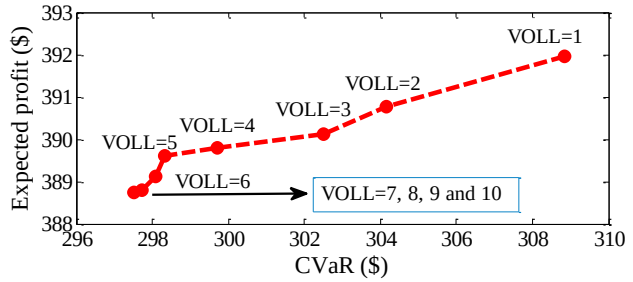

(b)

Fig. 7. *Expected profit versus CVaR for different VOLL values and $\beta = 0.01$*
(a) without DR and **(b)** with DR

Moreover, the expected profit, total cost of scheduled reserves, cost of MLS with respect to the total load and cost of ELNS versus VOLL are depicted in Table 4. This table shows that the reliability of the microgrid and the expected profit of the operator is largely dependent on the VOLL, especially in case without DR actions. The microgrid operator can choose a proper amount of VOLL to keep the microgrid reliable in order to face the unpredictable variability of renewable generations and load consumption. As can be seen from the same table, in case without DR support, when VOLL increases due to an increment in EENS, the expected profit decreases, severely. However, in case of incorporating DR actions, the expected profit has small variations once VOLL is increasing. As it can be observed from the table, with DR support, when VOLL is increased up to 8 $/kWh, no MLS occurs during the entire scheduling horizon. As a result, in higher values of the VOLL in which the total scheduled reserve and the ELNS remain constant, the expected profit remains almost unchanged. Moreover, with active participation of customers in DR, a part of up- and down-SR are allocated by responsive loads and consequently, the amount of these reserves provided by DGs decrease in case of with DR. However, the amount of non-SR is increased by DR participate, since, when the DR is considered, the microgrid uncertainties are increased and more non-SR is required, while responsive loads does not able to provide this type of reserve. Table 5 provides the total amount of spinning (SR) and non-spinning reserves (non-SR) allocated by DG and DR resources for different values of VOLL in the 24 hours' time scheduling. There is no doubt that the equilibrium point between energy, reserve and EENS can be changed by increasing the VOLL values. In other word, with increasing the VOLL, additional SR would be more economic than the MLS. Thus, as can be observe from the table, the amount of up- and down-SR increase in higher value of VOLL. The lowest value of scheduled reserves is attained for VOLL = 1 $/kWh.

In order to investigate the effect of VOLL on the reserve with details, the hourly up-SR provided by DG units and responsive loads for VOLL = 1 $/kWh and VOLL = 5 $/kWh is shown in Fig. 8. As can be seen, sum of up-SR (provided by both DGs and DR) increases for higher value of VOLL to accommodate the uncertainties and to reduce the load shedding events. In case with DR with considering uncertainty of responsive loads more reserve is required, which is partly provided by DG units as non-SR. Therefore, as can be observe in this figure the amounts of up-SR increase in some hours in case with DR actions.

Table 4 Expected profit and reliability level versus VOLL

VOLL	Expected profit ($)		Cost of total scheduling reserves ($)				MLS with respect to the total load (%)		Cost of EENS ($)	
			No DR		With DR					
	No DR	With DR	by DGs	by DR	by DGs	by DR	No DR	With DR	No DR	With DR
1	288.20	395.06	142.00	0	111.42	41.14	60.56	2.24	60.56	2.24
2	227.73	390.77	146.23	0	112.10	42.56	57.05	0.60	114.11	1.20
3	168.44	390.23	147.22	0	112.70	42.92	55.09	0.42	165.27	1.27
4	109.24	389.81	148.19	0	112.89	43.15	53.45	0.35	213.80	1.39
5	50.04	389.43	149.17	0	112.98	43.35	52.07	0.29	260.35	1.45
6	-9.02	389.12	150.12	0	113.20	43.40	51.34	0.23	308.04	1.40
7	-67.91	388.81	151.05	0	113.32	44.18	50.08	0.12	350.56	0.82
8	-126.61	388.73	151.87	0	113.74	44.62	49.41	0	395.28	0
9	-185.31	388.73	152.59	0	113.74	44.62	49.41	0	444.69	0
10	-241.22	388.73	153.14	0	113.74	44.62	49.41	0	494.10	0

Table 5 Impact of VOLL on the total scheduled reserve.

Case	VOLL ($/kWh)	Up-SR of DGs	Down-SR of DGs	Non-SR of DGs	Up-SR of DR	Down-SR of DR
Without DR	1	738	2401	1174	0	0
	5	801	2411	1309	0	0
	10	844	2419	1358	0	0
With DR	1	589	1404	1422	149	1136
	5	626	1404	1439	210	1140
	10	631	1404	1456	250	1144

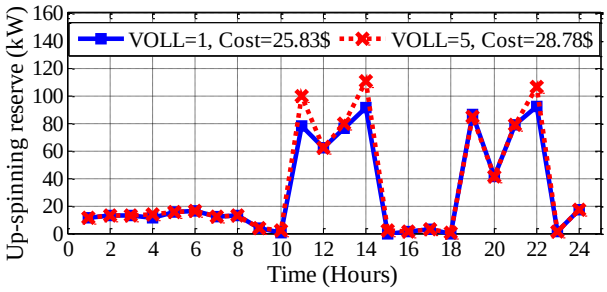

(a)

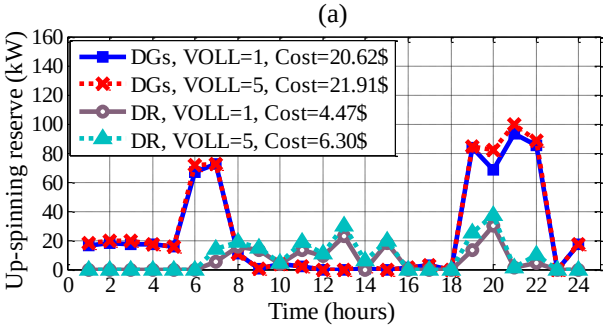

(b)

Fig. 8. *Hourly up-SR of DG units and responsive loads in* $\beta = 0.01$
(a) without DR and **(b)** with DR.

Table 6 depicts more numerically details about the expected profit of the microgrid operator, total cost of scheduled reserves, cost of EENS and the MLS with respect to the total load in different values of the risk aversion parameter β. As can be seen, when risk aversion increases, the total cost of scheduled reserves is increased in both cases. Moreover, the operator should allocate more reserve from the resources to have less forced load shedding encountering with undesired scenarios. Also, by increasing β, the percentage of MLS over the entire scheduling horizon is decreased due to more reserves allocated by resources. As a result, when risk aversion increases, although the expected profit of operator decreases, the microgrid will be more reliable under uncertainties.

To evaluate the effect of risk aversion parameter β on the scheduled reserve, the total amount of different types of reserve is illustrated in Table 7 for three values of β in VOLL=1 $/kWh. As can be seen, in the higher value of β, the amount of total scheduled reserve increases to reduce the load shedding in undesired scenarios. Hence, without DR support when risk aversion increase from 0.01 to 2, up-, down- and non-SR increase 11.8%, 0.56%, and 24%, respectively. However, when responsive loads participate in up/down SR, providing of these types of reserves from DGs decrease, especially in down-SR. To deploy down-SR customers should be committed and increase their consumption. Hence, they are more desired to participate in this type of reserve and therefore, the down-SR of DGs reduces in case with DR, significantly.

For better illustration, the hourly up-SR in two cases for β = 0.01 and β = 2 is shown in Fig. 9. As observed, the amount of reserve allocated by both DGs and DR at β = 2 is more than reserve at β = 0.01 in some hours. In an attempt to curb likely MLS events in some hours, the amount of reserve scheduled in the optimization problem increases by increasing parameter β. It should be noted that, although there is not much difference in reserve allocation during most of the times in a day, in some hours (i.e., 11:00, 13:00 and 14:00 in case without DR), which is likely to cause MLS, the amount of scheduled reserve increases when the risk aversion increases. In other words, MLS is applied only at some hours and in some undesirable scenarios and if the operator wants to become more risk averse (choosing higher β values), it should allocate more reserves in those hours. Therefore, there are no noticeable improvements in the results for the rest of hours.

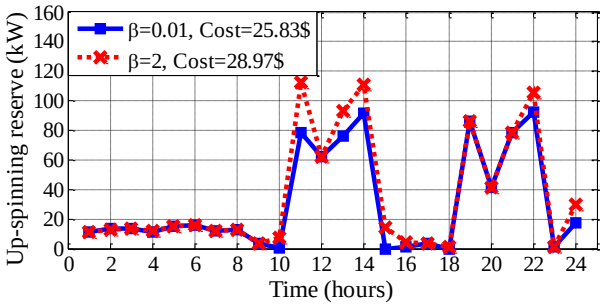

(a)

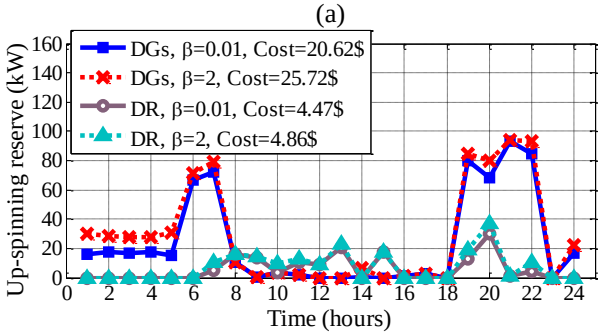

(b)

Fig. 9. *Hourly up-SR of DG units and responsive loads in VOLL=1 $/kWh,* **(a)** without DR and **(b)** with DR.

Fig. 10 shows that how the cost of EENS varies by increasing β in VOLL=1 $/kWh and VOLL=5 $/kWh with and without DR. The decrement in the expected cost of EENS is due to the reduction of load shedding actions in contingencies. As expressed before, when DR is considered, contribution of responsive loads in peak periods leads to a reduction in MLS and consequently a significant reduction in the cost of EENS (more than 95% for all β values). However, in case without DR support, cost of EENS for VOLL=1 $/kWh and VOLL=5 $/kWh is reduced to 10.7% and 19%, respectively. But, these values in case with DR are about 42% and 77%, respectively. In VOLL=5 $/kWh, although, the amount of MLS is reduced, increasing of VOLL causes the cost of EENS to be higher than that of in VOLL=1 $/kWh. Hence, by increasing β, the operator wants

Table 6 Expected profit and reliability level versus risk aversion parameter β.

β	Expected profit ($)		Total cost of scheduled reserves ($)				MLS with respect to the total load (%)		Cost of EENS ($)	
			No DR		With DR					
	No DR	With DR	Provided by DGs	Provided by DR	Provided by DGs	Provided by DR	No DR	With DR	No DR	With DR
0.01	57.71	389.43	147.39	0	112.99	43.35	56.87	0.29	284.34	1.45
0.01	57.42	389.13	148.44	0	112.06	45.51	56.51	0.16	282.56	0.81
0.50	57.15	385.78	149.67	0	110.76	53.02	56.14	0.12	280.70	0.62
1.00	56.38	379.83	150.98	0	110.14	62.48	55.77	0.09	278.87	0.46
1.50	55.41	375.30	152.53	0	109.57	69.54	55.41	0.07	277.04	0.37
2.00	54.88	373.32	153.89	0	109.69	71.67	55.10	0.06	275.52	0.32

to become more risk averse and purchase more reserves in some undesired scenarios. Therefore, by active participation of customers in DR program, the cost of EENS reduces with a higher rate. In such condition, additional scheduled reserve would be more cost-effective than interrupting the loads. Thus, in higher values of β the quantity of scheduled reserve will increase, while the cost of EENS decreases.

Table 7 Impact of the parameter β on the total scheduled reserve.

Case	Value of risk aversion (β)	Up-SR of DGs	Down-SR of DGs	Non-SR of DGs	Up-SR of DR	Down-SR of DR
Without DR	β =0.01	738	2411	1174	0	0
	β =0.5	792	2419	1375	0	0
	β =2	825	2425	1451	0	0
With DR	β =0.01	589	1422	1422	149	1136
	β =0.5	696	1369	1439	155	1408
	β =2	735	1348	1456	162	2028

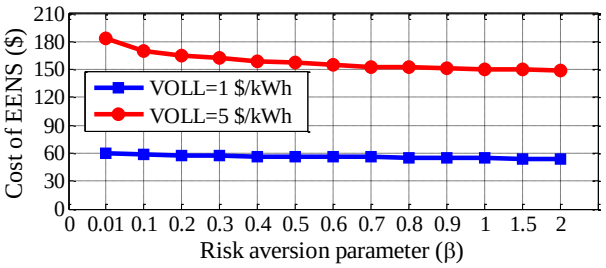

(a)

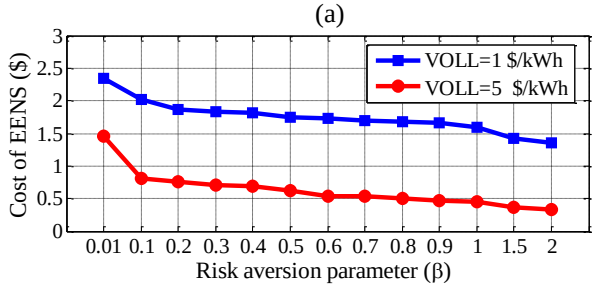

(b)

Fig. 10. *Cost of EENS under different risk aversion values* **(a)** without DR and **(b)** with DR.

6. Conclusions

In this paper, a risk-constrained stochastic framework was presented to maximize the expected profit of microgrid operator under uncertainties associated with the wind and PV power and also load demand. CVaR approach was used to model tradeoff between maximizing the operator's expected profit and the risk of getting low profits in undesired scenarios. The impacts of different values of VOLL and risk aversion parameter on the optimal solution of the proposed optimization problem have been investigated in two cases namely with and without DR. The summary of the numerical results are as the below:

- With participation of responsive loads in DR programs the system uncertainties increase which in turn necessitate more reserve allocation in higher VOLL and β values.
- By increasing VOLL and β values, the MLS in undesired scenarios is reduced and consequently, the expected profit of operator is decreased but the CVaR is increased. When VOLL varies from 1 to 10 $/kWh, a reduction of 187.4% and 24.1% can be seen in the expected profit in case of without and with DR support, respectively.
- With the support of responsive loads in peak periods through LC/LS mechanisms, the MLS and consequently the cost of EENS is decreased substantially (more than 96% for VOLL =1 $/kWh).

Future efforts will be mainly focused on the application of the proposed model for multi-microgrids with different types of consumers (e.g., residential, industrial, commercial). More investigations will also be conducted on uncertainty of components availability and load in the proposed model.

References

[1] Anvari-Moghaddam, A., Monsef, H., Rahimi-Kian, A. 'Cost-Effective and Comfort-Aware Residential Energy Management under Different Pricing Schemes and Weather Conditions', Energy and Buildings, 86, pp. 782-793, 2015.

[2] Anvari-Moghaddam, A., Guerrero, J.M., Vasquez, J.C., et al.: 'Efficient Energy Management for a Grid-Tied Residential Microgrid', IET Gener. Transm. & Distrib., 2017, 11(11), pp. 2752-2761.

[3] Moshari, A., Ebrahimi, A., Fotuhi-Firuzabad, M.: 'Short-Term Impacts of DR Programs on Reliability of Wind Integrated Power Systems Considering Demand-Side Uncertainties,' IEEE Trans. on Power Syst., 2016, 31, (3), pp. 2481-2490

[4] Yang, S., Zeng, D., Ding, H., C., et al.: 'Stochastic security-constrained economic dispatch for random responsive price-elastic load and wind power,' IET Renewable Power Generation, 2016, 10, (7), pp. 936 – 943.

[5] Parvizimosaed, M., Farmani, F., Monsef, H., Rahimi-Kian A., 'A multi-stage Smart Energy Management System under multiple uncertainties: A data mining

approach', Renewable Energy, 102-A, pp. 178-189, 2017.
[6] Aghaei, J., Alizadeh, M.I., Abdollahi, A., Barani, M.: 'Allocation of demand response resources: toward an effective contribution to power system voltage stability', IET Gener. Transm. Distrib., 2016, 10(16), pp. 4169-4177
[7] M. Vahedipour-Dahraie, H. R. Najafi, A. Anvari-Moghaddam, et al.: ' Study the Effect of Time-Based Rate Demand Response Programs on Stochastic Day-Ahead Energy and Reserve Scheduling in Islanded Residential Microgrids', Appl. Sci. 2017, 7 (4), 378, pp. 1-19
[8] Gholami, A., Shekari, T., Aminifar, F., Shahidehpour, M.: 'Microgrid Scheduling with Uncertainty: The Quest for Resilience', IEEE Trans smart grid 2016, 30(3), pp. 1337-1350
[9] Moshari, A., Ebrahimi, A., Fotuhi-Firuzabad, M.: 'Short-Term Impacts of DR Programs on Reliability of Wind Integrated Power Systems Considering Demand-Side Uncertainties', IEEE Trans on Power Syst. 2016, 31(3), pp. 2481-2490
[10] Aghaei. J., Alizadeh, M.I., Siano, P., Heidari, A., 'Contribution of emergency demand response programs in power system reliability', Energy, 2016, 103, pp. 688-696
[11] Aghaei, J., Nikoobakht, A., Sian, P., Nayeripour, M., Heidari, A., Mardaneh, M., 'Exploring the reliability effects on the short term AC securityconstrained unit commitment: A stochastic evaluation', Energy, 2016, 114, pp. 1016-1032
[12] Wang, J., Shahidehpour, M., Li, Z., 'Security-constrained unit commitment with volatile wind power generation', Power Syst IEEE Trans. 2008, 23, pp. 1319-27
[13] Moghaddam, I.G., Nick, M., Fallahi, F., et al.: 'Risk-averse profit-based optimal operation strategy of a combined wind farm-cascade hydro system in an electricity market', Renew. Energy, 2013, 55, pp. 252–259
[14] Shayeghi, H., Sobhani, B.: 'Integrated offering strategy for profit enhancement of distributed resources and demand response in microgrids considering system uncertainty,' Energy Conv. Manage., 2014, 87, pp. 765–777
[15] Anderson, C.L., Cardell, J.B.: 'A decision framework for optimal pairing of wind and demand response resources', IEEE Systems Journal, 2012, 29, (1), pp. 149–159
[16] Garcia-Bertrand, R.: 'Sale prices setting tool for retailers', IEEE Trans. Smart Grid, 2013, 4, (4), pp. 2028–2035
[17] Carrion, M., Philpott, A.B., Conejo, A.J., et al.: 'A stochastic programming approach to electric energy procurement for large consumers', IEEE Trans. Power Syst., 2007, 22, (2), pp. 744–754
[18] Wang, H., and Jianwei H.: 'Joint investment and operation of microgrid', IEEE Trans. Smart Grid, 2017, 8 (2), pp. 833-845
[19] Rashidizaheh-Kermani, H., Vahedipour-Dahraie, M., Najafi, H.R., et al.: 'A Stochastic Bi-Level Scheduling Approach for the Participation of EV Aggregators in Competitive Electricity Markets', Appl. Sci. 2017, 7, pp. 1-16
[20] Vahedipour-Dahraie, M., Rashidizaheh-Kermani, H., Najafi, H.R., et al.: 'Stochastic Security and Risk-Constrained Scheduling for an Autonomous Microgrid with Demand Response and Renewable Energy Resources', IET Renewable Power Generation, 2017, 11(14), pp. 1812-1821.
[21] Conti, S., Nicolosi, R., Rizzo, S.A., Zeineldin, H.H.: 'Optimal dispatching of distributed generators and storage systems for MV islanded microgrids', IEEE Trans. Power Deliv., 2012, 27, (3), pp. 1243–1251
[22] Choudhry, M.: 'An Introduction to Value-at-Risk', John Wiley & Sons, Third edition, 2006.
[23] Rockafellar, R.T., Uryasev, S., 'Conditional value-at-risk for general loss distributions', Journal of Banking & Finance, 2002, 26 (7), pp. 1443–1471
[24] Nguyen, DT., Le, LB., 'Risk-Constrained Profit Maximization for Microgrid Aggregators with Demand Response', IEEE Transactions on smart grid, 2015, 6, (1), pp. 135-146
[25] Zh, D., Nilay, S., Lazaros, P.: 'Efficient energy consumption and operation management in a smart building with microgrid', Energy Convers Manag., 2013, 74, pp. 209-222
[26] Mollahassani-pour, M., Abdollahi, A., Rashidinejad M.: 'Investigation of Market-Based Demand Response Impacts on Security-Constrained Preventive Maintenance Scheduling', IEEE Systems Journals 2015, 9(4), pp. 1496-1506
[27] Damousis, I.G., Bakirtzis, A.G., Dokopolous, P.S.: 'A solution to the unit-commitment problem using integer coded genetic algorithm', IEEE Trans. Power Syst., 2004, 19(2), pp. 1165-1172.
[28] Eyvindson K., and Kangas A., 'Evaluating the required scenario set size for stochastic programming in forest management planning: incorporating inventory and growth model uncertainty', Can. J. For. Res., 46, pp. 340–347, 2016.
[29] Arthur, D., Vassilvitskii, S.: 'K-means++: The advantages of careful seeding', in Proc. 18th Annu. ACM-SIAM Symp Discrete Algorithms (SODA '07), New Orleans, LA, USA, 2007, pp. 1027-1035
[30] Wang, J., Shahidehpour, M., Li, Z., 'Security-constrained unit commitment with volatile wind power generation', IEEE Trans. Power Syst., 2008, 23, pp. 1319-1327
[31] Rezaei, N., Kalantar, M.: 'Stochastic frequency-security constrained energy and reserve management of an inverter interfaced islanded microgrid considering demand response programs', Int. J. Electr. Power Energy Syst., 2015, 69, pp. 273–286
[32] Vahedipour-Dahraie, M., Rashidizaheh-Kermani, H., Najafi, H.R., et al.: 'Coordination of EVs Participation for Load Frequency Control in Isolated Microgrids', Appl. Sci. 2017, 7(6), 539, pp. 1-16.
[33] Rezaei, N. Kalantar, M.: 'Smart microgrid hierarchical frequency control ancillary service provision based on virtual inertia concept: An integrated demand response and droop controlled distributed generation framework', Energy Conversion and Management 2015, 92, pp. 287-301
[34] 'The General Algebraic Modeling System (GAMS)

Software', online available at: http://www.gams.com, accessed on 15 September 2016